JOURNAL OF AIRCRAFT
Vol. 31, No. 6, November–December 1994

Further Analysis of High-Rate Rolling Experiments of a 65-Deg Delta Wing

Lars E. Ericsson*
Mt. View, California 94040
and
Ernest S. Hanff†
Institute for Aerospace Research, Ottawa, Ontario, Canada

Further analyses have been performed of the experimental results obtained in the roll oscillation tests of a 65-deg sharp-edged delta wing at 30-deg inclination of the roll axis in order to uncover the fluid mechanical phenomena causing the unusual, highly nonlinear vehicle dynamics. It was found in an earlier analysis that in addition to the expected effect of convective flow time lag, the test results show highly nonlinear effects on vortex breakdown of the oscillatory rate. The present analysis reveals that these effects are themselves influenced by convective flow time lag. As a result, the past time history of the oscillatory response can in some cases have a strong influence on the final trim condition.

Nomenclature

b = wing span
c = wing root chord
f = oscillation frequency
k = reduced frequency, $\omega b/2U_\infty$
L = lift: coefficient, $C_L = L/(\rho_\infty U_\infty^2/2)S$
l = rolling moment: coefficient, $C_l = l/(\rho_\infty U_\infty^2/2)Sb$
N = normal force: coefficient, $C_N = N/(\rho_\infty U_\infty^2/2)S$
p = aerodynamic pressure: coefficient, $C_P = (p - p_\infty)/(\rho_\infty U_\infty^2/2)$
S = reference area, projected wing area
t = time
U = horizontal velocity
$\bar{U}$ = convection velocity
W = vertical velocity
x = axial body-fixed coordinate, Fig. 8
y = spanwise body-fixed coordinate, Fig. 8
z = vertical body-fixed coordinate, Fig. 8
α = angle of attack
Δ = increment or amplitude
Δt = time lag
$\Delta\phi$ = roll oscillation amplitude
θ_{LE} = leading-edge half-angle
Λ = leading-edge sweep angle, $\pi/2 - \theta_{LE}$
ξ = dimensionless x coordinate, x/c
ρ = air density
σ = inclination of body axis
ϕ = roll angle
ϕ_0 = mean roll angle
$\dot{\phi}$ = reduced roll rate, $\dot{\phi}b/2U_\infty$
ω = angular frequency, $2\pi f$

Subscripts
c = critical
LE = leading edge
max = maximum
V = vortex
VB = vortex breakdown
∞ = freestream conditions

Differential symbols
C_{l_ϕ} = $\partial C_l/\partial\phi$
$\dot{\phi}$ = $\partial\phi/\partial t$

Presented as Paper 93-0620 at the AIAA 31st Aerospace Science Meeting and Exhibit, Reno, NV, Jan. 11–14, 1993; received Sept. 19, 1993; revision received March 28, 1994; accepted for publication April 6, 1994.

*Engineering Consultant. Fellow AIAA.
†Senior Research Officer. Member AIAA.

Introduction

IN a recently completed analysis of how to include agility considerations in the design of fighter aircraft,[1] the following conclusion is drawn: "The rank order of agility payoff functions placed torsional agility first, followed by axial agility and pitch agility." Consequently, it is of utmost importance to be able to predict the unsteady aerodynamics of rapid roll maneuvers.

Results obtained in high-rate, large-amplitude roll oscillation tests[2] of a sharp-edged 65-deg delta wing at 30-deg inclination of the roll axis are unique in that they cannot be obtained by time-lagging static experimental results.[3,4] This is contrary to past experience showing that the dynamic effects of separated flow on bodies of revolution[5] and slender wings[6] could be predicted simply by phasing the force or moment vector measured in static tests to account for the effect of convective flow time lag. The present tests show that there is in addition an effect of the roll-induced velocities at the leading edge, which can change the magnitude of the force or moment vector. A hypothesis was presented in Ref. 3 that could explain some of the unusual experimental results obtained on a 65-deg delta wing. This article is a follow-up of that analysis, aimed at extending it to include other unique experimental results not discussed in Refs. 3 and 4.

Analysis

In order to make this article comprehensible without requiring the reading of Refs. 3 and 4, the more significant results discussed in the earlier analysis will be recapitulated. Only the results obtained for roll oscillations around $\phi_0 = 0$, at σ = 30-deg inclination of the body-fixed roll axis of the 65-deg delta wing,[2,7] will be discussed. The static rolling moment exhibits highly nonlinear characteristics in the range -10 deg $< \phi <$ 10 deg (Fig. 1). The almost discontinuous change of the rolling moment in Fig. 1 is caused by the breakdown of the leading-edge vortices.

Figure 2a shows how the breakdown of delta-wing leading-edge vortices occurs first at the trailing edge of the delta wing,

and progresses forward as the angle of attack is increased.[8] At nonzero roll angle, the angle of attack and effective leading-edge sweep of the delta wing are[3,4]

$$\alpha(\phi) = \tan^{-1}(\tan\sigma\cos\phi) \quad (1)$$

$$\Lambda(\phi) = \Lambda \pm \tan^{-1}(\tan\sigma\sin\phi) \quad (2)$$

The effective sweep of the wing half that rolls upward (lee-side wing half) increases, and that of the other decreases (see Fig. 2b), resulting in an aft and forward shift, respectively, of the corresponding vortex breakdown locations. Figure 2a shows that the forward movement of the vortex breakdown on the windward side will be very modest, compared to the rapid aft movement for the leeward side. When accounting for the beveled leading edge[9] the effective angle of attack is less than 30 deg. For such an α value Fig. 2a indicates that the vortex breakdown would rapidly move from roughly mid-chord to the trailing edge on the leeward wing when the effective sweep approaches $\Lambda = 70$ deg. A critical sweep angle $\Lambda \approx 69$ deg is indicated by the dashed line in Fig. 2b. Considering the wing areas affected by the movement of the vortex breakdown, one can see that the effect of the breakdown movement on the rolling moment is almost entirely generated by the leeward wing half, where the increased vortex lift generates a highly nonlinear, statically destabilizing change of the rolling moment. Representing this by a discontinuous C_l change when $\Lambda = 69$ deg is exceeded gives the C_l characteristics represented by a solid line in Fig. 1. For the sake of simplicity, this idealized representation of the static characteristics will be used in the discussion that follows.

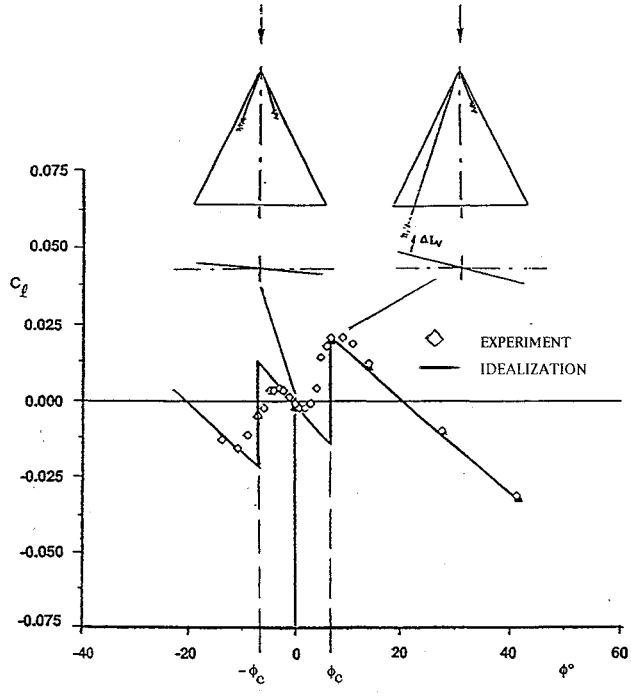

Fig. 1 $C_l(\phi)$ characteristics at $\sigma = 30$ deg.[7]

In order to understand the dynamic characteristics, it is beneficial to first examine the delta wing roll dynamics in the absence of vortex breakdown.[10] One important characteristic of the dynamic loading induced by leading-edge vortices is the effect of convective time lag. When the angle of attack is changed in a stepwise manner, the new vortex starts developing at the apex and grows in the downstream direction[11] (Fig. 3). Thus, a time lag $\Delta t = x/\bar{U}_V$, where $\bar{U}_V \geq U_\infty$ occurs before the new vortex has been established at station x. The same type of time-lag effect is realized for a change of roll angle. The static effect is to increase the vortex-induced lift on the windward wing half, as illustrated for $\phi = \Delta\phi(t - \Delta t)$ in Fig. 3. A corresponding lift decrease occurs on the leeward side. That is, the effect is statically stabilizing. However, due to the time-lag effect, the rolling delta wing will experience this vortex-induced lift increment ΔL_V at time t, when the roll angle is zero, $\phi = 0$ (see Fig. 3). That is, the vortex-induced lift-increment is dynamically destabilizing. This opposition between static and dynamic stability effects is the general result of time lag.[5,6]

Figure 4 illustrates how such a time lag would cause the $C_l(\phi)$ characteristics, obtained by changing the roll angle at a constant rate, to lag the idealized static $C_l(\phi)$ characteristics (solid line). Figure 5 shows how the measured $C_l(\phi)$ characteristics for the reduced roll rate $\bar{\phi} = 0.05$, obtained from large amplitude roll oscillations, varied with the roll angle.[2] The measured dynamic characteristics demonstrate that ap-

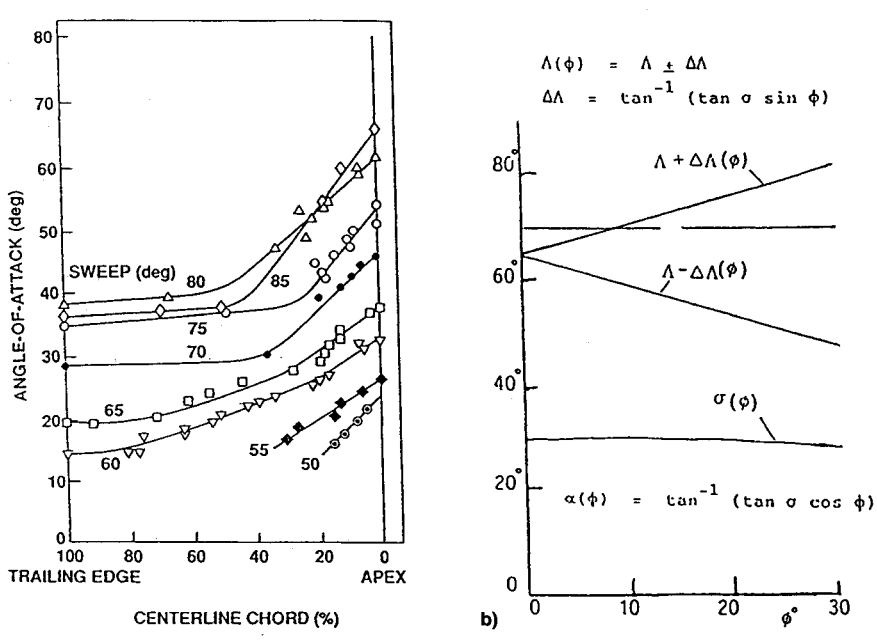

Fig. 2 Static vortex breakdown characteristics: a) vortex breakdown position on sharp-edged delta wings[8] and b) effect of roll angle on effective leading-sweep and angle of attack.

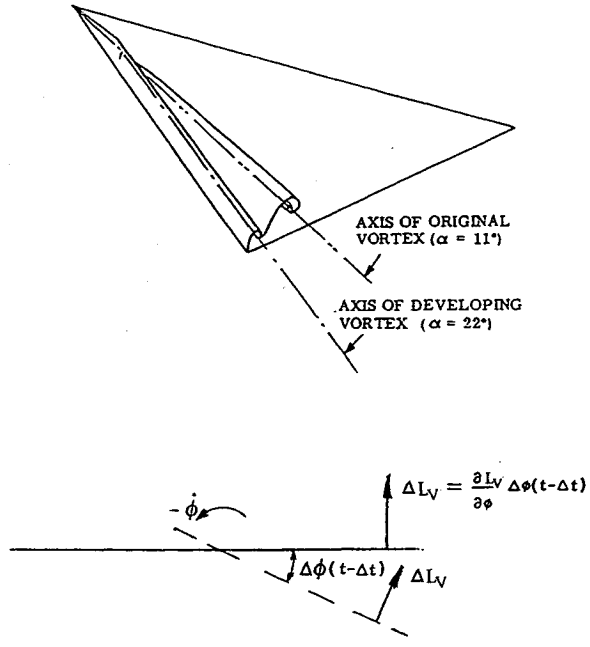

Fig. 3 Formation of leading-edge vortex and generation of incremental vortex-induced lift after stepwise change of angle of attack.[11]

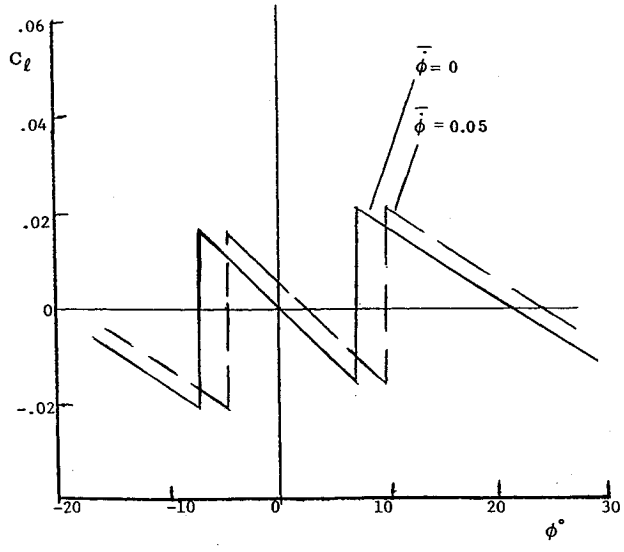

Fig. 4 Expected effect of convective time lag on $C_l(\phi)$ characteristics.

plying the time-lag effect to the separation-induced static characteristics is not sufficient for prediction of the experimental dynamic characteristics. The results indicate that the magnitude of the vortex-induced rolling moment is changed from its static value. A well-known example of similar motion-induced effects is the large dynamic-stall overshoot of static lift maximum.[12,13] In that case the pitching motion changes the effective geometry through pitch-rate-induced accelerated-flow and moving-wall effects. A similar roll-rate-induced change of the effective geometry seems to be present for the 65-deg, sharp-edged delta wing, having a large effect on the lift and the associated rolling moment.

The effect of longitudinal camber on the breakdown of the leading-edge vortex on a slender delta wing is large[14] (Fig. 6). For the same maximum local angle of attack on the delta wing α_{max}, a positive camber of $\Delta\alpha/\alpha_{max} = 1$ causes breakdown to occur downstream of the trailing edge, whereas a negative camber of the same magnitude, $\Delta\alpha/\alpha_{max} = -1$, causes burst to occur very close to the apex.

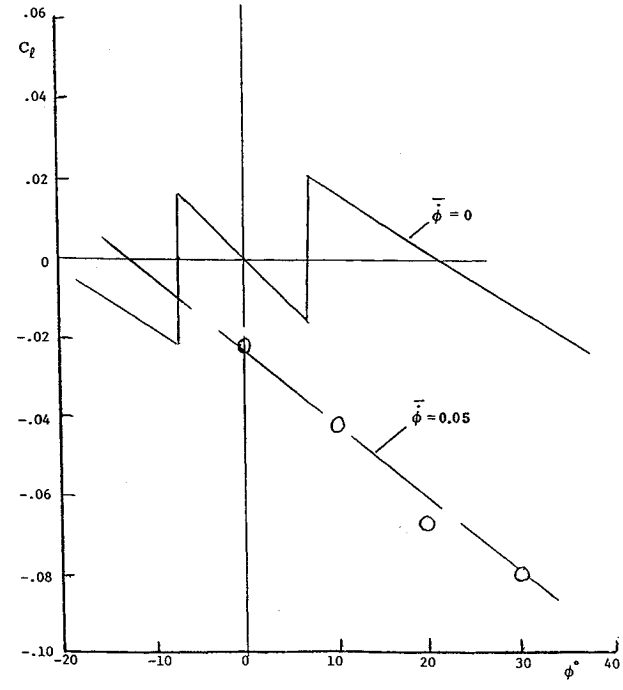

Fig. 5 Measured effect of positive constant roll rate on $C_l(\phi)$ characteristics.

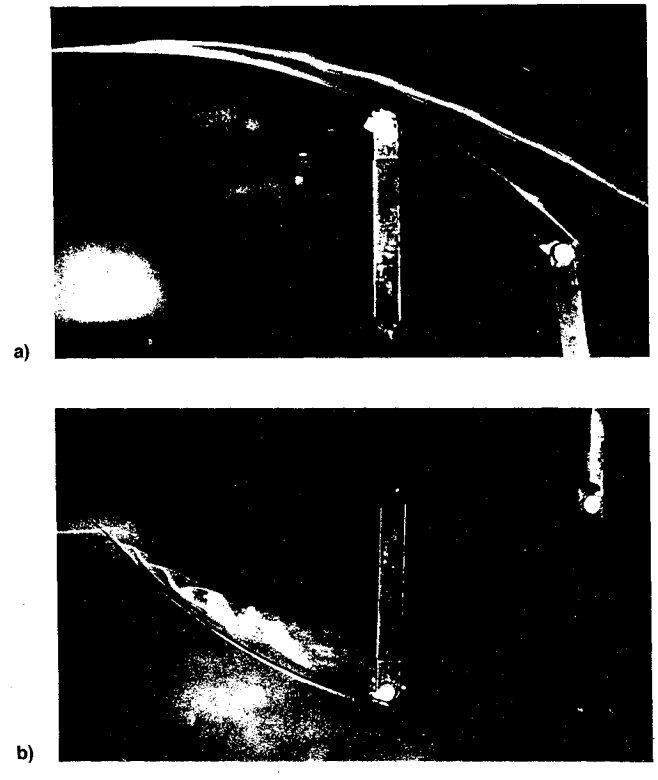

Fig. 6 Effect of longitudinal camber on vortex breakdown on an 80-deg delta wing.[14] Local incidence a) increasing and b) decreasing with distance from apex.

Obviously, for a pitching delta wing the pitch-rate-induced camber will have similarly large effects on the breakdown of leading-edge vortices. It is shown in Ref.15 that the nonlinear lift characteristics of delta wings are determined by the ratio between the angle of attack and the leading-edge half-angle, the parameter being $\tan\alpha/\tan\theta_{LE} \approx \alpha/\theta_{LE}$, where $\theta_{LE} = \pi/2 - \Lambda$. The roll-stability derivative C_{l_ϕ} is, of course, also determined by this parameter,[15] and it was suggested in Ref.

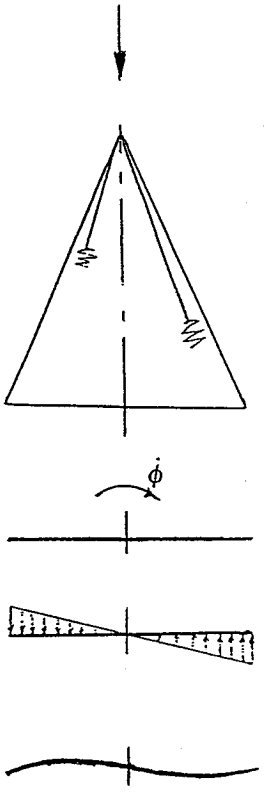

Fig. 7 Roll-rate-induced conical camber.

16 that the local α/θ_{LE} variation from apex to trailing edge would be very important, and that as a consequence, the roll-rate-induced camber effect would be very similar to the pitch-rate-induced camber effect. In both cases, it is the motion-induced change of the local angle of attack at the leading edge that matters (Fig. 7).

The local, roll-rate-induced, conical camber is

$$\Delta\alpha_{LE} = \tan^{-1}(W_{LE}/U_\infty \cos\alpha) \approx \dot{\phi}\xi \sec\alpha \qquad (3)$$

Thus, the total roll-rate-induced camber at the trailing edge is

$$\Delta\alpha_{LE} = \dot{\phi} \sec\alpha \qquad (4)$$

where

$$|\dot{\phi}| = k\Delta\phi \qquad (5)$$

At $\phi = \phi_0 = 0$, $\alpha = \sigma = 30$ deg. That is,

$$\Delta\alpha_{LE} = 2k\Delta\phi/\sqrt{3} \qquad (6)$$

Thus, $|\Delta\alpha_{LE}| \leq 9.2$ deg for $k \leq 0.2$ and $\Delta\phi \leq 40$ deg. This gives a ratio $\Delta\alpha_{LE}/\alpha = 0.31$ for $\alpha = 30$ deg. This ratio is comparable in magnitude to the ratio $|\Delta\alpha|/\alpha = 1$, which produced the huge effects on vortex breakdown shown in Fig. 6.

Discussion

Following the suggestion in Ref. 3, static tests were performed with models deformed to produce the roll-rate-induced camber[17] (Fig. 8). In order to keep the leading-edge sweep unchanged, the equivalent static model was made to have the leading edge in one plane, resulting in equations for the static equivalent deformation that are more complicated than Eqs. (3–6). The test results were as expected.[3] That is, the twisted-up side of the delta wing experienced later vortex

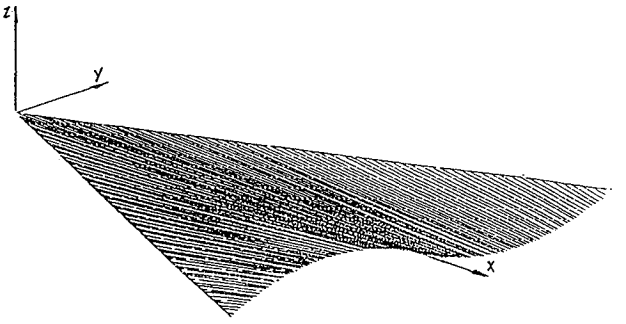

Fig. 8 Thin-sheet model, deformed to represent the maximum roll-rate-induced camber.[17]

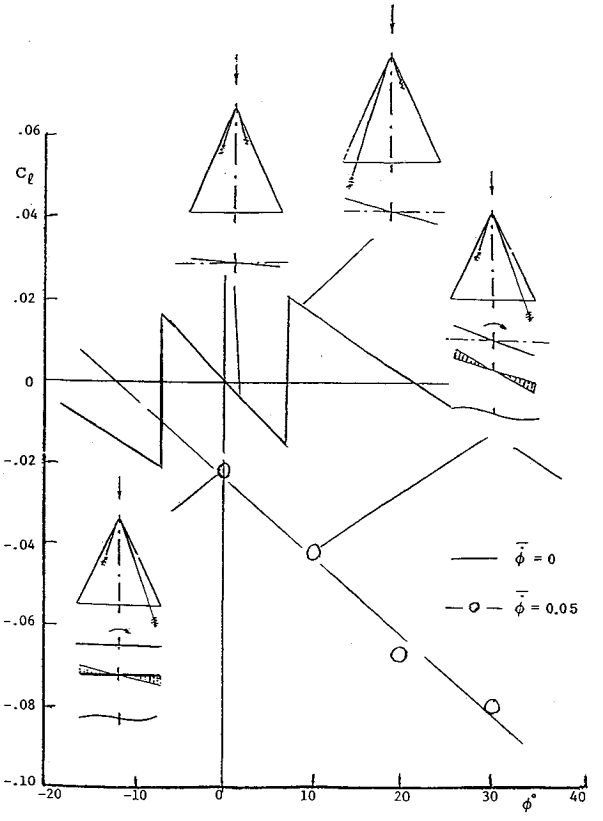

Fig. 9 Effect on $C_l(\phi)$ characteristics of rampwise increase of the roll angle, $\dot{\phi} = 0.05$.

breakdown than the opposite, twisted-down side, $\xi_{VB} \approx 0.70$, compared to $\xi_{VB} \approx 0.45$ (at $\phi = 0$) for one test case.

For the positive roll rate in Fig. 5, the roll-rate-induced camber delays vortex breakdown on the downstroking, and promotes it on the upstroking wing half. For $\dot{\phi} = 0.05$, the effect was apparently large enough to prevent the breakdown from moving downstream of the trailing edge on the port wing and upstream of it on the starboard wing (see sketches in Fig. 9). This explains why the statically destabilizing rolling-moment-discontinuities never materialized under the dynamic conditions. Aside from the effect of these discontinuities, the difference between the $C_l(\phi)$ characteristics for $\dot{\phi} = 0.05$ and $\dot{\phi} = 0$ is the combined effect of time lag and roll-rate-induced apparent mass.[10]

Applying the same reasoning to $\dot{\phi} = -0.05$ as for $\dot{\phi} = 0.05$ in Fig. 9, one gets the inset sketches shown in Fig. 10, according to which no vortex breakdown did occur on the leeward wing half. This is in agreement with the experimental data trend. That is, the $C_l(\phi)$ characteristics for $\dot{\phi} = -0.05$ are essentially those for $\dot{\phi} = 0$ and $\phi > 10$ deg, modified by the combined effects of time lag and apparent mass.[10]

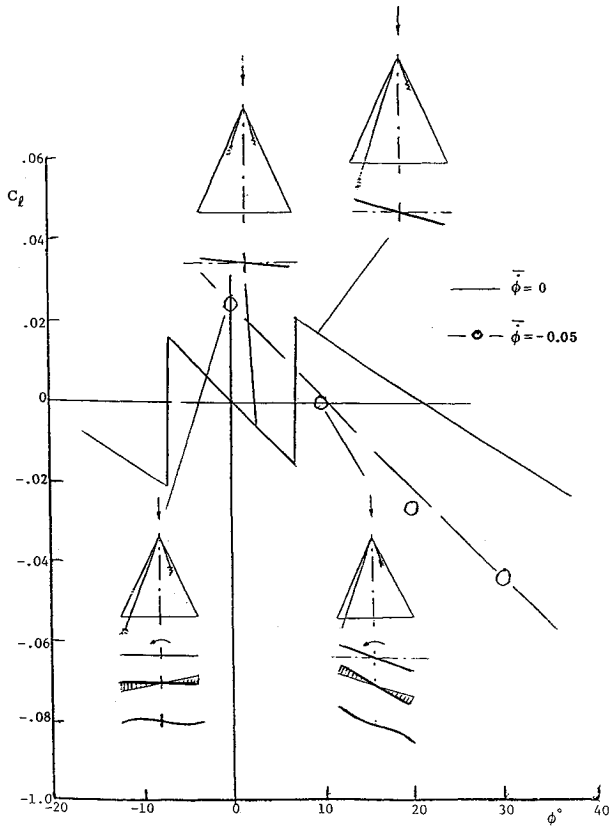

Fig. 10 Effect on $C_l(\phi)$ characteristics of rampwise decrease of the roll angle, $\dot{\bar{\phi}} = -0.05$.

An assessment of the time lag can be obtained from the unsteady pressure measurements, giving the results shown in Figs. 11a and 11b.[7] In Fig. 11c it is illustrated how a time lag, giving a phase lag of less than 90 deg, $\omega\Delta t < \pi/2$, is indicated by the experimental results. That is, the maximum roll-rate-induced camber, generated at $\phi = 0$ for $\dot{\phi} < 0$, would be realized a time Δt later at $\phi = -\dot{\phi}\Delta t$. The experimental results in Fig. 11b show the suction peak to be located between $\phi \approx -10$ deg and $\phi \approx -40$ deg. The flatness of the suction peak is largely the result of the small change of the roll rate around $\phi = 0$ in Fig. 11c. Neglecting the effect of the roll-rate-induced camber and ascribing the difference between the measurements for $k = 0$ and $k = 0.14$ to the effect of time lag alone would give $0.58 < U_\infty \Delta t/c < 5.25$ for 10 deg $< \omega\Delta t < 90$ deg, corresponding to -10 deg $> \phi > -40$ deg in Fig. 11b.

That the time lag had to be of significant magnitude was indicated by the test results for $C_l(\phi)$ at $\phi_0 = 0$ and $\dot{\phi} = 0$ (Fig. 12). The data show that as the roll rate is increased, causing vortex breakdown to be delayed more and more on the downstroking windward side (Fig. 10), the aerodynamic stiffness is increasing towards that existing in the absence of vortex breakdown.[10] The reason for this residual roll-rate effect at $\dot{\phi} = 0$ is the time lag Δt and corresponding phase lag $\omega\Delta t$ in the response of the vortex breakdown to the roll-rate-induced camber at $\dot{\phi} > 0$ (see Fig. 12b). Figure 13 illustrates how the past time history differs for $\dot{\phi} > 0$ compared to $\dot{\phi} < 0$, for positive roll angles $\phi > 0$. The experimental results in Figs. 9 and 10 for $\dot{\bar{\phi}} = 0.05$ and $\dot{\bar{\phi}} = -0.05$, respectively, do not show any distinct effects of this difference in past time histories. They look very much as if they were obtained for (rampwise) roll-angle changes at constant rates. A more extensive analysis, possibly with an extended data base, is needed before one can determine how the effect of past time history depends upon $\Delta\phi$ and k.

Some guidance can be obtained from past experience with dynamic airfoil stall.[12] The dynamic overshoot of static lift maximum remains the same if the reduced pitch rate $\dot{\alpha}c/U_\infty$ is simulated at the critical point, the static stall angle. That is, the dynamic lift overshoot will in that case remain the same for oscillatory and rampwise changes of the angle of attack. Thus, in the present case one could expect that the reduced roll rate $\dot{\phi} = \dot{\phi}b/2U_\infty$ at the critical point,[18] $|\phi_c| < 10$ deg in Fig. 1, is the important simulation parameter. As in the case of dynamic stall,[12] the sufficiency of this simulation is probably limited to large amplitude oscillations, where the time histories around the critical point(s) are similar for rampwise and oscillatory angular changes. The experimental results shown in Figs. 9 and 10 are for large amplitude oscillations around $\phi_0 = 0$, explaining the rampwise C_l characteristics.

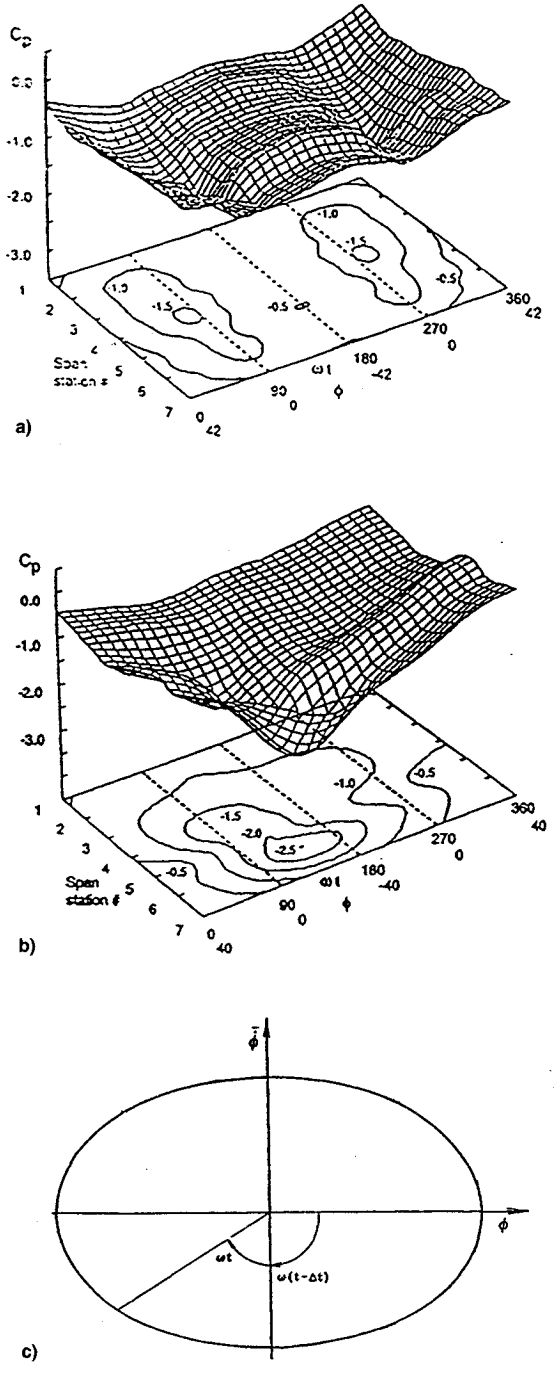

Fig. 11 Instantaneous top-surface pressures at 75% of center chord as affected by the oscillation frequency: a) $\phi_0 = 0$, $\Delta\phi = 42$ deg, $k = 0$[7]; b) $\phi_0 = 0$, $\Delta\phi = 40$ deg, $k = 0.14$[7]; and c) ϕ and $\dot{\phi}$ as functions of ωt.

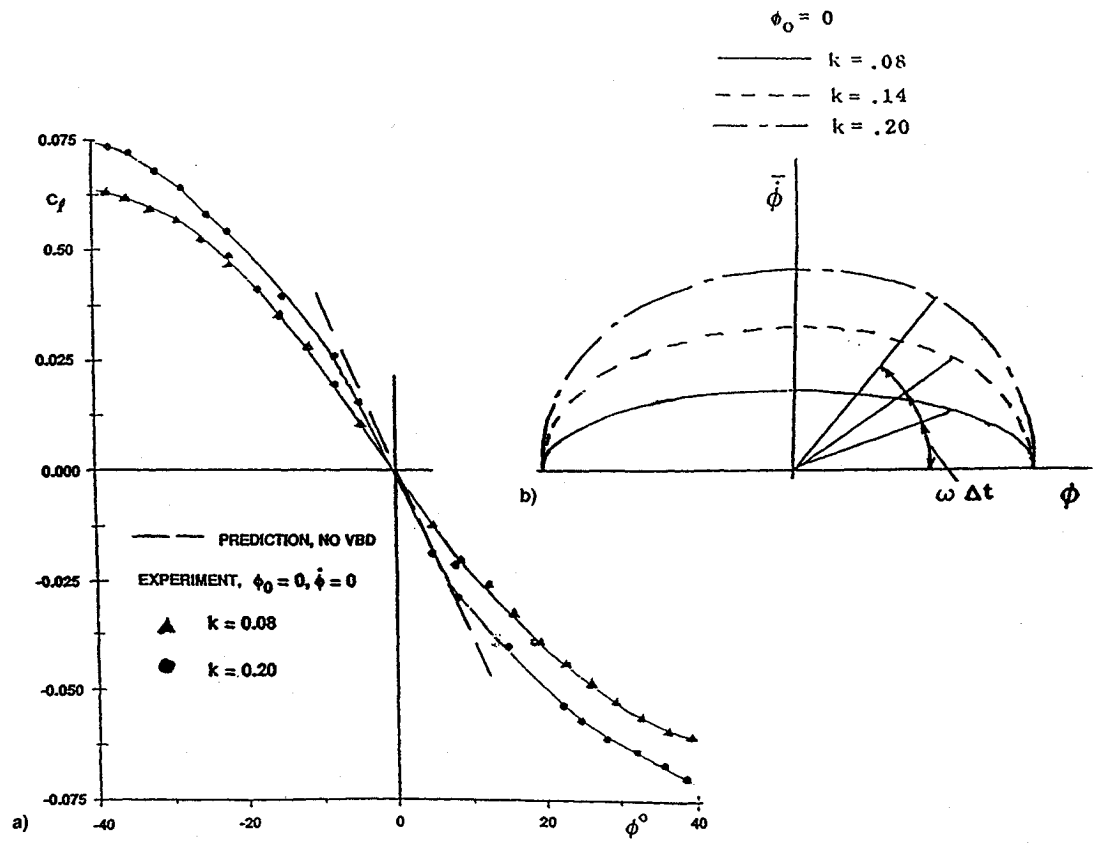

Fig. 12 Effect of roll rate on measured $C_l(\phi)$ characteristics: a) $C_l(\phi)$ at $\phi_0 = 0$ and $\dot{\phi} = 0$ for various reduced frequencies and b) effect of time lag on residual roll-rate effect at $\dot{\phi} = 0$ for insignificant roll acceleration changes.

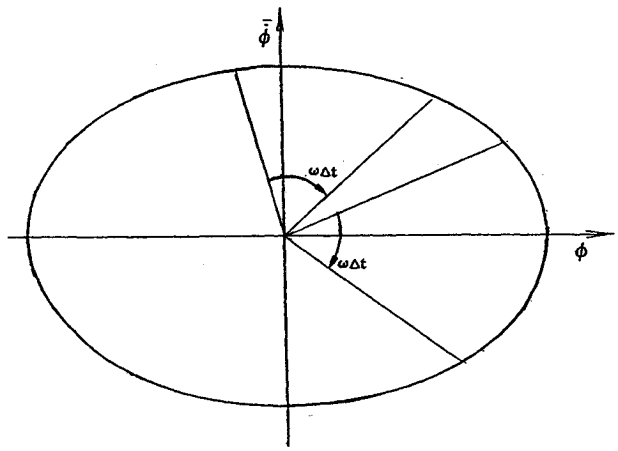

Fig. 13 Effect of time lag on residual roll-rate effect.

When the critical point ϕ_c falls near the end of either the upstroke or downstroke of the oscillatory change of ϕ, one expects the past time history to play an important role, which it appears to do in determining the final trim condition for the free-to-roll releases[7] (Figs. 14 and 15). Already the results in Fig. 14 raised some unanswered questions in regard to how the rolling wing selected the final trim point. The results in Fig. 15 appear at first even more mystifying, especially before one has studied the results in Figs. 11–13. The reversal of $\phi(t)$ at $t \approx 0.2$ s towards the final trim at $\phi \approx 20$ deg appears to be the result of the past time history of the type illustrated in Fig. 13 for $\phi = 0$. Such a reversal can apparently occur near the critical state ($\phi = \phi_c$), where the roll-rate-induced camber and time history effects are large. These results demonstrate that the final trim point depends strongly upon the past roll time history.

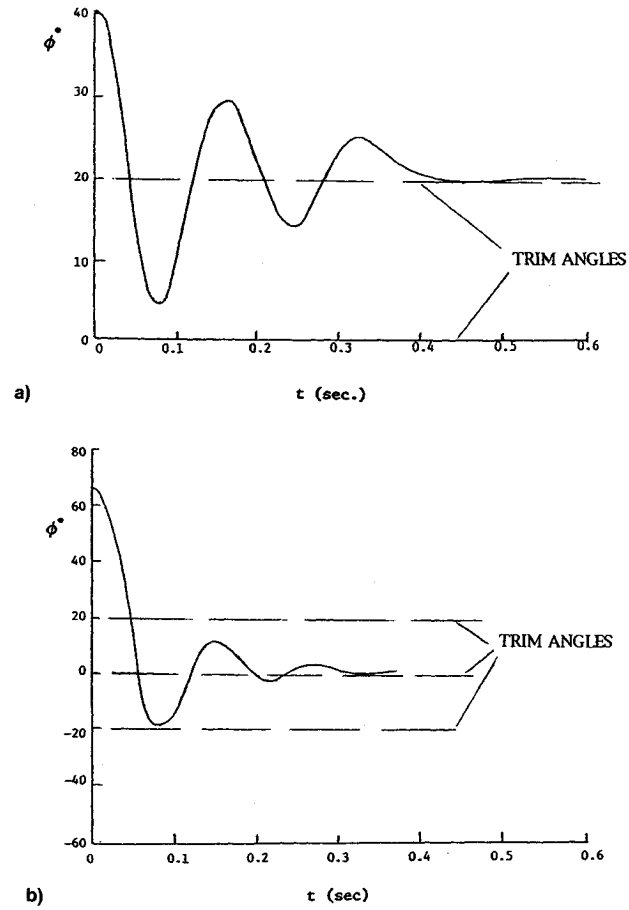

Fig. 14 Free-to-roll motion time histories. Initial roll angle $\phi(0)$ = a) 41 and b) 66 deg.

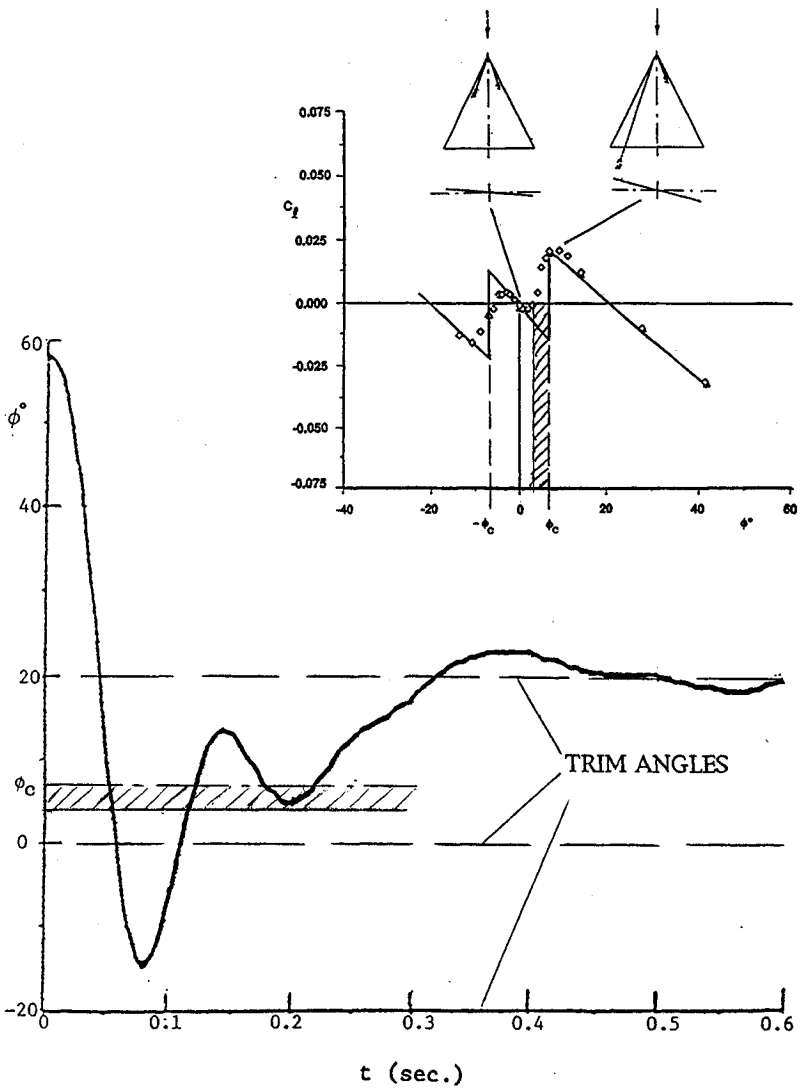

Fig. 15 Free-to-roll motion time history for release at $\phi(0)$ = 59 deg.

Conclusions

Further analysis of the highly nonlinear roll dynamics observed in high-frequency, large-amplitude roll oscillation tests of a sharp-edged 65-deg delta wing at a roll-axis inclination of 30 deg has led to the following conclusions.

1) Static and dynamic roll characteristics are dominated by the effect of vortex breakdown.

2) The dynamic effect of vortex breakdown is to a large extent controlled by the roll-rate-induced conical camber.

3) The aerodynamic response to both roll angle and roll rate is subject to significant convective time-lag effects. As a consequence, the final trim point for the free-to-roll releases will often be dependent upon the past roll time history.

Acknowledgments

This article is based upon results obtained under a joint research program of the U.S. Air Force Office of Scientific Research, Wright Laboratory, the Institute for Aerospace Research, and the Canadian Department of National Defense.

References

[1]Skow, A. M., "Agility as a Contributor to Design Balance," *Journal of Aircraft*, Vol. 29, No. 1, 1992, pp. 34–46.

[2]Hanff, E. S., and Jenkins, S. B., "Large-Amplitude High-Rate Roll Experiments on a Delta and Double Delta Wing," AIAA Paper 90-0224, Jan. 1990.

[3]Ericsson, L. E., "Analysis of Wind-Tunnel Data Obtained in High-Rate Rolling Experiments with Slender Delta Wings," Inst. for Aerospace Research, IAR-CR-14, National Research Council, Ottawa, Canada, Aug. 1991.

[4]Ericsson, L. E., and Hanff, E. S., "Unique High-Alpha Roll Dynamics of a Sharp-Edged 65 deg Delta Wing," *Journal of Aircraft*, Vol. 31, No. 3, 1994, pp. 520–525.

[5]Ericsson, L. E., and Reding, J. P., "Fluid Dynamics of Unsteady Separated Flow, Part I, Bodies of Revolution," *Progress of Aerospace Sciences*, Vol. 23, 1986, pp. 1–84.

[6]Ericsson, L. E., and Reding, J. P., "Fluid Dynamics of Unsteady Separated Flow, Part II, Lifting Surfaces," *Progress of Aerospace Sciences*, Vol. 24, 1987, pp. 249–356.

[7]Hanff, E. S., and Ericsson, L. E., "Multiple Roll Attractors of a Delta Wing at High Incidence," Paper 31, AGARD-CP-494, July 1991.

[8]Wentz, W. H., and Kohlman, D. L., "Vortex Breakdown on Slender Sharp-Edged Wings," *Journal of Aircraft*, Vol. 8, No. 3, 1971, pp. 156–161.

[9]Ericsson, L. E., and King, H. H. C., "Effect of Leading-Edge Cross-Sectional Geometry on Slender Wing Unsteady Aerodynamics," *Journal of Aircraft*, Vol. 30, No. 5, 1993, pp. 793–795.

[10]Ericsson, L. E., and King, H. H. C., "Rapid Prediction of High-Alpha Unsteady Aerodynamics of Slender-Wing Aircraft Dynamics," *Journal of Aircraft*, Vol. 29, No. 1, 1992, pp. 85–92.

[11]Lambourne, N. C., Bryer, D. W., and Maybrey, J. F. M., "The Behavior of the Leading Edge Vortices over a Delta Wing Following a Sudden Change of Incidence," Aeronautical Research Council, R&M 3645, UK, March 1969.

[12]Ericsson, L. E., and Reding, J. P., "Fluid Mechanics of Dynamic

Stall, Part I, Unsteady Flow Concepts," *Journal of Fluids and Structures*, Vol. 2, No. 1, 1988, pp. 1–33.

[13]Harper, P. W., and Flanigan, R. E., "The Effect of Rate of Change of Angle of Attack on the Maximum Lift of a Small Model," NACA TN 2061, 1949.

[14]Lambourne, N. C., and Bryer, D. W., "The Bursting of Leading-Edge Vortices—Some Observations and Discussion of the Phenomenon," Aeronautical Research Council, R&M 3282, UK, April 1961.

[15]Ericsson, L. E., and Reding, J. P., "Approximate Nonlinear Slender Wing Aerodynamics," *Journal of Aircraft*, Vol. 14, No. 12, 1977, pp. 1197–1204.

[16]Ericsson, L. E., and Reding, J. P., "Unsteady Aerodynamic Analysis of Space Shuttle Vehicles. Part II: Steady and Unsteady Aerodynamics of Sharp-Edged Delta Wings," NASA CR-120123, Aug. 1973.

[17]Hanff, E. S., and Huang, X. Z., "Prediction of Leading-Edge Vortex Breakdown on a Delta Wing Oscillating in Roll," AIAA Paper 92-2677, June 1992.

[18]Jenkins, J. E., Myatt, J. H., and Hanff, E. S., "Body-Axis Rolling Motion Critical States of a 65-Degree Delta Wing," AIAA Paper 93-0621, Jan. 1993.